Routledge
Taylor & Francis Group

Transportation Planning and Technology

ISSN: (Print) (Online) Journal homepage: www.tandfonline.com/journals/gtpt20

A dynamic evaluation of an underground transportation system using image processing and centrality index computation

Lorenzo Mussone, Valeria J. Aranda Salgado & Roberto Notari

To cite this article: Lorenzo Mussone, Valeria J. Aranda Salgado & Roberto Notari (16 Sep 2024): A dynamic evaluation of an underground transportation system using image processing and centrality index computation, Transportation Planning and Technology, DOI: 10.1080/03081060.2024.2403643

To link to this article: https://doi.org/10.1080/03081060.2024.2403643

Published online: 16 Sep 2024.

TRANSPORTATION PLANNING AND TECHNOLOGY
https://doi.org/10.1080/03081060.2024.2403643

Routledge
Taylor & Francis Group

A dynamic evaluation of an underground transportation system using image processing and centrality index computation

Lorenzo Mussone[a], Valeria J. Aranda Salgado[a] and Roberto Notari[b]

[a]Department ABC, Politecnico di Milano, Milano, Italy; [b]Department of Mathematics, Politecnico di Milano, Milano, Italy

ABSTRACT

The study of transportation networks covers a wide range of topics related to managing services and maintaining structures. In order to represent the topological structure of such a network, we associated a graph to a network. Then some different properties or attributes of the network can be managed as weights to be applied to the graph itself. In addition, different centrality indices can be computed in order to identify nodes or edges that are more important or more exposed to capacity changes (such as, for example, disruptive events). The purpose of this research is to provide a methodology for dynamically evaluating the significance of stations in a transportation network. This is accomplished through two distinct phases of activity. Firstly, we propose a dynamic analysis of the underground transportation system of the city of Milan, Italy. This transportation system is the mobility backbone of the city and counts four lines with 110 links and 107 stations, including 21 junctions (the transfer stations that connect the lines). Two data sets about passenger flows (both entering and leaving stations) are used to calculate the flows on links with a resolution of 1 min. The data sets refer to a week in 2018, without the changes in demand due to the pandemic scenario. Data are processed through an ad hoc written assignment procedure. Secondly, a centrality index is calculated by using passenger flows (entering, exiting, and on-segments) as weights of the underground graph. After maps reporting the outcomes of those calculations are drawn, an image comparison is carried out by using image processing tools and different aggregation intervals, in order to investigate how the importance or exposure of each station changes over time. The findings demonstrate that over time, indices vary by station, with junction stations naturally having the highest values. By increasing the observation interval from 1 min up to 30 min, index changes become progressively smoother, like an application of a low pass filter, suggesting that for certain applications (e.g. those concerning security), aggregating data could lead to misleading conclusions.

ARTICLE HISTORY
Received 25 October 2023
Accepted 6 September 2024

KEYWORDS
Underground networks evaluation; flow assignment; centrality index; dynamic analysis; image processing

CONTACT Lorenzo Mussone lorenzo.mussone@polimi.it Department ABC, Politecnico di Milano, P.za L. da Vinci, 32, Milano 20133, Italy

1. Introduction

To understand the behaviour and functionality of underground networks, it is undoubtedly interesting and helpful to first analyse their topology. Actually, just like in every other transportation system, the interaction between supply and demand determines the operational state, whether in equilibrium or dynamically. Therefore, incorporating demand and supply (topology included) into a unique framework allows a comprehensive description of the functionality of the network. The questions above can be summarized as: 'How can the train scheduling be changed to avoid saturation of train capacity?'

Then, one of our aims is to find stations and links that are more exposed to failures or operating reductions because of the large load on them. On the other hand, we would like to get information on the performance of a network in case of disruption. This aim can be obtained from the computation of the values a centrality index takes at a station or at a link when we use passenger loads as weights.

To highlight the limitations when taking only the topology into account, it is pretty obvious that a station, line, or train that serves a large number of passengers is more essential than those that serve fewer people. This may alter the order in which the investigation's key components are ranked when looking at the network topology only.

Another aspect is that demand fluctuates throughout the course of the day. Therefore, in order to obtain all the information required for managing and controlling the transportation network, a time-dependent analysis must be carried out. Finding a suitable time period is undoubtedly a difficult task because it must ensure that the results are complete while the calculation burden is kept to a minimum.

In this paper, we developed a general methodology to get a description of an underground network that incorporates supply and demand. The data we need at the very beginning are the graph of the network, the passenger flow entering and exiting the network by hour per day, and the Origin-Destination (OD) matrix depending on time. As an example, we apply this methodology to Milan underground network. Actually, the methodology can be applied to all types of transportation networks, provided that all passenger flows (entering and exiting the stops) are known as well as the scheduled service.

Of course, because results depend on the specific demand for quantity, time, and OD distribution, those presented here are strictly related to the Milan case study.

When computing the values of a centrality index in dependence on time, we have the issue of representing, analysing and comparing them. To address these issues, we created a tool based on graphical image comparison to provide an easy synthesis of the numerous computations performed.

We base our methodology on the plausible assumptions listed below for this kind of transportation system:

- congestion is not considered, even though platforms and trains can be extremely crowded during rush hours;
- the route from station A to station B is selected according to the timetable of the rush hour service; of course, travel time can change over time according to the actual service;
- each passenger chooses its own route based on the shortest time needed;

- train timetable is completely respected;
- the times from turnstiles to platforms and vice versa, and for transfers from one line to another, are deterministic and computed by the service provider; and
- passenger counts are accurate and error-free.

The demand considered in this research is from a week in 2018 and consists of datasets containing the flow of passengers entering and leaving the stations of Milan underground network. For this data, it is necessary to perform a trip assignment in order to allocate each passenger (accessing the station) to a specific route that will take them to their final destination (the leaving stations). We construct the OD matrix from automated fared data, collected from the service provider. Once every passenger is assigned to a route, we compute the load on each edge of the graph, depending on time, so to get a dynamical picture of the working network. We then use the computed loads as weights on edges and compute a centrality index with the aim of finding the most exposed nodes of the graph to disruptions. We analyse the changes in the values of the index by means of an image comparison.

The paper develops into four other sections. Section 2 provides an overview of the literature on simulation models and their applications, as well as on centrality indices, definitions, and applications. Section 3 lists and describes the computing tools and datasets used in the research. Section 4 analyses and discusses the results. Finally, Section 5 draws the conclusions.

2. Literature review

Because the proposed methodology is based on one side on the analysis of entering and exiting flows and on the scheduled service, and on another side on the use of centrality indices, we propose a literature review on both issues, and so we have two subsections, one for each.

2.1. Simulation and data processing

To put our study in the right research context, we briefly resume some papers on related topics, from the OD matrix construction, to the analysis of flow in some underground networks and the study of the vulnerability of such networks.

For the OD matrix construction, it was usual to conduct surveys. More recently, some researchers have used smart card data (Automated Fare Collection, AFC), station entry, observed counts (e.g. see Lam, Wu, and Chan 2003), and traffic counts (see (Wong et al. 2005) among the many research papers on the same topic) on different transportation modes in order to construct it and allocate passengers to a specific route.

Cui (2006) used AFC data to construct an OD matrix using a seed matrix and marginal values to form single OD routes, applying iterative proportional fitting and maximum likelihood estimations. In this approach, there are three steps to estimating the OD matrix: (1) Number of ridership, seed matrix, and transit flows; (2) iterative proportional fitting (IPF), seed matrix, and access/egress number; (3) data to localise transfers. Kuhlman (2015) constructed a likely OD matrix from AFC data. We remark that the data used do not provide the entering and the exiting station for the same passenger but

only the total amount of entering and exiting quantity per station. Ait-Ali and Elíasson (2019) used a model based on a constrained entropy maximization approach, using datasets from weekdays divided into 15 min each. After the OD matrix has been created, it is 'proved' through the aggregated travel statistics from the service provider. Mohammed and Oke (2023) reviewed more than 30 studies using different sorts of data sets with the aim of constructing an OD matrix that can help in the assignment of the public transport demand. The reviewed works suggested that there are many possibilities to do the demand assignment depending on the information and the methodology available. Chiang et al. (2017) analysed the passenger flow and recommended ways to alleviate crowding and congestion. They gathered qualitative and quantitative data, through interviews with London Underground employees, CCTV observation, and the analysis of customer satisfaction data.

As an alternative or in parallel to the OD matrix definition, passenger flow can be simulated. For instance, Stoilova and Stoev (2015) developed a methodology for simulating passenger flow in an underground station using a direct-event approach. Hong, Li, and Zhu (2017) proposed a methodology for assigning passenger flows on a metro network based on AFC data and realized timetable. The paper by M'Cleod et al. (2017) addressed the topic of transportation network vulnerability within the context of the New York City subway system by using an approach based on shortest-path passenger flow simulations in order to quantify delays experienced by passengers arising from disruptive events. Zhang et al. (2021) proposed a hierarchical modelling framework for passenger flow prediction. It includes two layers of fuzzy models, where a global model is used to predict for ordinary circumstances and a number of local models is used to predict variations in passenger numbers due to specific factors, such as events and weather.

From the perspective of passenger movements inside the stations (crowding problem), entering and exiting flows must be analysed. The study by Loukaitou-Sideris, Taylor, and Turley (2015) aimed to understand the particular factors that affect and may constrain passenger queuing, and to identify and evaluate practises for efficient, expedient, and safe passenger flows in different types of stations and during rush hours and atypical (e.g. evacuation) situations. Liu and Chen (2019) first analysed the surveillance video during rush hours in some typical metro stations and obtained the critical parameters of pedestrian motion in metro stations. Moreover, they proposed a 'destination choice model' and 'path planning algorithm' to simulate passenger choices in underground stations.

Xu, Mao, and Bai (2016) used the trip data obtained from the Beijing Subway System to characterize passenger temporal patterns and then to build a directed weighted passenger flow network. In (Hu et al. 2017), the authors incorporated the load of metro networks and passenger volume into the analysis of network features. Section load was selected as an edge weight to demonstrate the influence of ridership on the network and a weighted calculation method for complex network indicators and robustness was proposed to capture the unique behaviours of a metro network. The proposed method was applied on the Beijing Subway. The passenger volume in terms of the daily OD matrix was extracted from exhausted transit smart card data.

The paper by Wang, Ma, and Chan (2020) tried to overcome the restriction of earlier studies, where theoretical approaches have considered the topological characteristics and

the impact of disruptions in subway systems, but they had not been supported by empirical data. In their study, the authors used a data set containing 392 detailed records of disruptions to subway services in Beijing from 2011 to 2017 and came to the conclusion that factors from GIS data, operations, passenger flow, and the cause of disruptions must also be taken into account in order to accurately predict disruption effects.

2.2. Centrality index

The number of research topics on centrality indices' applications in transportation networks is vast; here, we simply highlight a small number of them through a few noteworthy contributions. It is important to keep in mind that each index considers the characteristics of the transportation network in a different way and is computed by means of a particular algorithm. As a result, depending also on the attributes (weights) taken into account, the index can highlight various local or global strengths or weaknesses of a network. E.g. some indices to assess the vulnerability of a network, can be obtained by applying topology-based indices with different inputs. As an example, travel cost can be used instead of the average shortest travel distance.

Traditional centrality indices are Degree, Closeness, Eigenvector and Betweenness centrality. Degree and Eigenvector centrality aim at measuring the attractiveness of each node, mainly from a topological point of view. Betweenness and Closeness are based on the number of nodes on the shortest paths between couples of nodes (Freeman 1978).

Derrible and Kennedy (2011) stated that while graph theory is employed in various fields, from computer science to physics, it began as a solution to an urban transportation problem. Derrible (2012) distinguished between transfer and terminal nodes, and between single and multiple edges. These ideas were proposed to look at the structure of transportation systems to figure out how directness (related to the length of shortest path between nodes) and complexity are related.

Wang and Cullinane (2016) utilized the centrality measures proposed by Opsahl, Agneessens, and Skvoretz (2010) to analyse the maritime transportation network. Wang et al. (2011) applied Degree, Closeness and Betweenness, on the air transportation network of China. (Wang, Antipova, and Porta 2011) examined the correlation between 'street centrality' and land use density in Baton Rouge, Louisiana. Street centrality is obtained through the application of Closeness, Betweenness, and Straightness centrality indices. Straightness index measures the connectivity between two points: the more straight the connection, the better the path. Tsiotas and Polyzos (2015) introduced a centrality index called 'Mobility Centrality' for analysing traffic flow in a road transportation network. They used this index to measure the propensity of each node to attract network flow. Cheng et al. (2015) proposed three new indices, Commuter Flow, Time Delay and Delay Flow Centrality in which the authors consider the commuter flow and the amount of delay induced to the passengers due to disruption at each node. In this way, they solve the problem of neglecting flow rate and delay by analysing the network performance. The formula of Commuter Flow Centrality for a disrupted node uses the number of commuters per hour affected by that disruption. Time Delay Centrality is defined as the time passengers will spend if they would take a different means to reach their destinations in case of disruption in that node. Delay Flow Centrality is calculated as the ratio

between Time Delay Centrality and the total commuter flow of the network. Chopra et al. (2016) presented a multi-pronged framework that analyses information on network topology, spatial organization and passenger flow to study the resilience of the London metro system. Guo and Lu (2016) proposed to apply the Neighbourhood Centrality, which aggregates the network centrality values in a geographic area. The neighbourhood eigenvector centrality (influence of the neighbouring rail stations) can explain for up to 79% of the variations in the age demographics, the choice in transportation mode, and the price and choice of housing.

According to Gu et al. (2020), the vulnerability of a transportation network can be examined by analysing the change in a specific quantitative index. The choice of the index for analysing the network vulnerability depends on the aim of the investigation since different indices evaluate vulnerability from different perspectives. They proposed two measures as examples of topology-based indices. The former quantifies the relative change in the average shortest distances between network nodes, the latter considers the reversed average distance between nodes of the network as a measure of efficiency of the network in conveying passengers.

Kumar et al. (2019) proposed a method to account for the most critical links considering daily functionality of the network, such as evacuation planning and emergency operations, when the closure of even one critical link can alter the whole circulation pattern significantly. They consider three factors for a criticality indicator: the link traffic volume, connectivity to important facilities, and number of origins and destinations crossing the link.

Complex network theory provides a different point of view (e.g. small world and scale free models) from which to explore the properties of transportation networks. Latora and Marchiori (2002) studied in detail the Boston underground network and proved that it has the 'small world' property. Later, in (Derrible and Kennedy 2010), the authors proved that metro networks are quite often both 'scale-free' and 'small world'. They also made suggestions on how to improve the robustness of such networks. Dimitrov and Ceder (2016) focused on the Auckland integrated public transportation network and proved that it is a mixture of 'scale-free' and 'exponential' networks.

Scott et al. (2006) proposed a new method based on a network robustness index to evaluate the performance of a transportation network. Wu et al. (2018) introduced a novel centrality index, the node occupying probability, and they used it to evaluate the robustness of metro networks. Jiang and Claramunt (2016) calculated network connectedness, average path length, and clustering coefficient to investigate city street networks. Newman (2001) proposed to calculate the average distance between each pair of nodes or the average path length as another technique to define the spread of a random network. In the same manner as the diameter, the average path length scales with the node number. Barthelemy (2004) applied betweenness centrality in large complex networks discovering that the nodes with a high betweenness would impose critical constraints on network security in real transportation systems. Alvarez-Socorro, Herrera-Almarza, and González-Díaz (2015) developed a global robustness index based on the inclusion-exclusion principle, a line coverage similarity measure comparable to network dissimilarity indices. Another index to evaluate the network robustness was defined in (Mussone, Aranda Salgado, and Notari 2024)

Each of the indices mentioned above will provide us with a variety of information about the topology of the network or other desirable aspects depending on the considered weights (but on edges only). Moreover, those indices enable us to rank the nodes of a network from different perspectives. However, the obtained results from these indices may also be misleading and may not reflect the node importance or an accurate comprehensive perspective of the network functionality. For example, Degree and Betweenness assign 1 and 0, respectively, to every terminal node. Hence, these two indices do not distinguish between different terminals, while, in underground networks, different terminal nodes have different importance. Closeness only depends on the weights of shortest paths, and so it does not take into account paths whose weight is greater than the minimum. Since such paths do play a role in the description of transportation networks, closeness, as it is, is not suitable for applications to transportation we want to consider. Mending the aforementioned deficiencies, new indices were proposed in Mussone, Viseh, and Notari (2020; 2022), one of which is Icentr used in this research. It has notable advantages and increases our capability for a more extensive investigation of transportation networks, particularly underground networks.

3. Materials and methods

In this section, we illustrate the many components and steps that form the methodology we propose. For the reader convenience, we summarize the methodology in the third subsection, and we explain the various parts in the other subsections.

3.1. The overall methodology

The research approach consists of the following steps:

- Data on passenger flows are examined and reviewed for consistency and missing data,
- The system's graph is created to calculate the centrality index,
- Divide hourly demand (the turnstiled data) into 1–10 min intervals,
- Assign demand to the network,
- Compute passenger flow to calculate centrality indices; and
- Evaluate outcomes using image processing.

3.2. The graph

Usually, the building of a graph associated to a transportation system requires some assumptions and interpretations. In the case of underground networks this task is simplified because of the regularity of their structure and because connections between two stations are generally in both directions. Therefore, the resulting graph generally has a symmetric adjacency matrix and can be treated and drawn as non-oriented.

The underground network of Milan has four lines (red M1, green M2, yellow M3, and lilac M5) at the years of the research; in 2022 the blue line M4 was inaugurated, even if

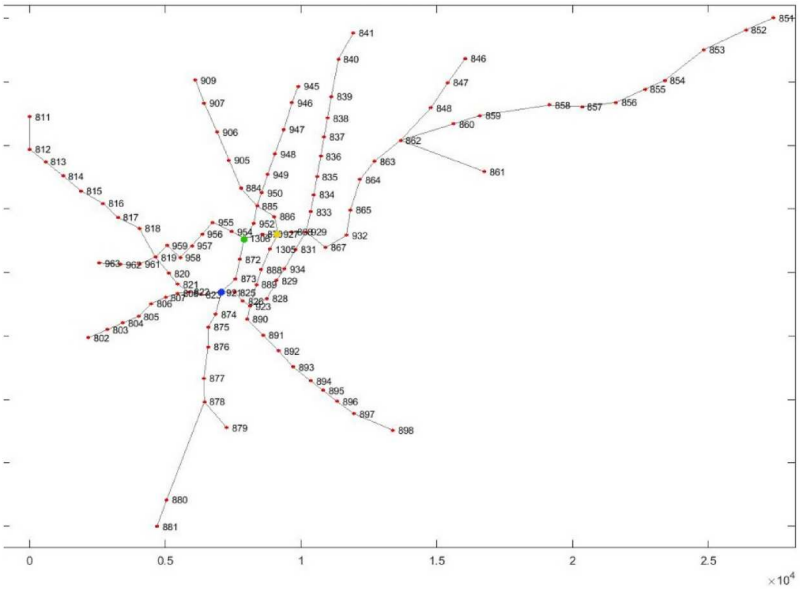

Figure 1. The complete graph of the underground network of Milan, Italy (the three main stations are identified by a different colour node: blue for Cadorna, green for Porta Garibaldi, and yellow for Centrale station).

not yet completed. In total, the four lines count 121 stations. Because different lines travel at different depths, some stations have direct connections between crossing lines, implying that they are the same transfer station (where lines cross) from a topological point of view. We define a transfer station as one that has a walkable, reasonably short, and internal link between two or more lines. At the end, the graph has 107 stations with 110 links. Figure 1 reports the complete graph of Milan underground network with the code used for each station. The structure has a central body, where the 4 lines cross, and many legs (10) leading to the terminal stations.

3.3. The data sets

Two data sets concerning passenger flows (for both access and egress – Entry and Exit – from stations) are used and pertain to the week of 9–15 April 2018 (a scenario prior the pandemic), specifically:

(1) Data from turnstiles ('Turnstiled'), aggregated by 1 h,
(2) Data from tickets ('Fared'), giving the time (in hours:minutes) the ticket was identified entering and exiting.

Table 1 summarizes some characteristics of the used data sets. The number of records reports the number of items in the data set that coincides with the passenger flow only for the Fared data set.

A comparison between Entry and Exit daily data for the whole network shows a difference of about 4% (entries are more than exits), which is considered physiological and due

Table 1. Characteristics of the main data sets used in the research.

File	No. records	Days	Time aggregation/ resolution	Content
Turnstiled (9–15 April 2018)	39,900	7 (a complete week)	1 h	Aggregated passenger flow
Fared (9–15 April 2018)	9,042,533	7 (a complete week)	1 min	Each passenger
Timetable (13–14–15 April 2018)	131,610	Friday (and all weekdays), Saturday, Sunday	1 s	Timetable for all trains

to many factors (illegal exits, not working or wrong turnstiles). Of course, this effect is not uniformly distributed among stations.

In Figure 2, some samples of the analysis on the time dependence of passenger flows, developed for all the stations, are drawn by showing the typical trends that can be observed (IN and OUT mean entry and exit curves, respectively; week and wend mean weekdays and weekend days, respectively).

On weekdays, the overall daily demand (on the days considered) is approximately 1,350,000 passengers, whereas on weekends it ranges between 550,000 and 850,000. There are two peak hours, one in the morning (in the range of 7:00–8:00) and one in the evening (in the range of 17:00–18:00). It can be observed that in some stations the presence of peaks depends on the type of flow under consideration (if entering or exiting). For example, in Figure 2(a), considering weekdays, the station of Duomo-Cordusio (in the city inner centre) has a peak hour for exiting flow only in the morning, and for entering flow only in the evening; whereas in Figure 2(b) the Centrale station exhibits the classical two peaks, one in the morning and one in the evening, both for exiting and entering flows. It is worth noting that the y-scales in Figure 2(a,b) are different. In addition, the analysis confirms the difference between weekdays and weekend days, not only for the total amount of counted passengers but also for the dynamics of their curves. The split of demand among lines is rather constant over a

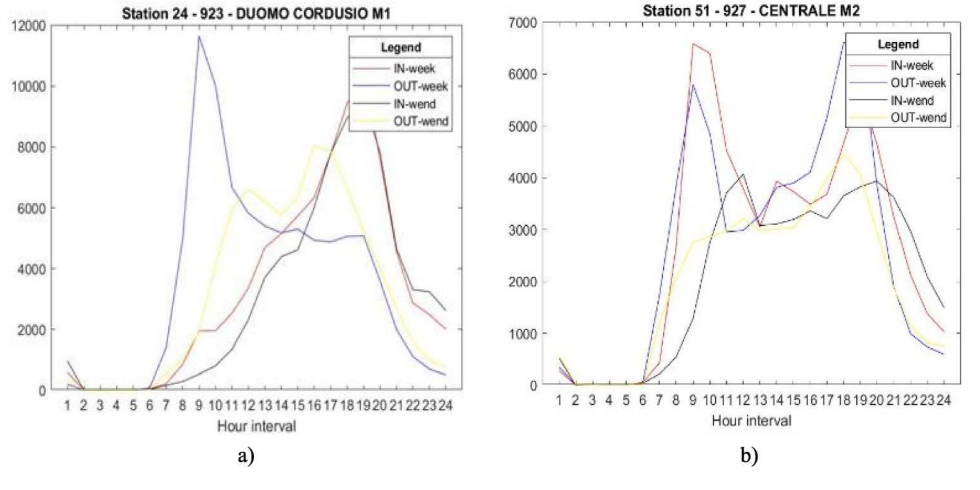

Figure 2. Two examples of passenger flow hourly curves for entries (IN) and exits (OUT) for weekdays (week) and weekend days (wend).

weekday, and it is 37%, 34%, 22%, and 7%, respectively, for the red M1, green M2, yellow M3, and lilac M5 lines.

3.4. The assignment procedure

In order to calculate the flow on edges an assignment procedure was carried out. In Figure 3 the schematic layout is drawn and in Figure 4 the list of functions developed for the task is reported.

We assumed that there were no trips lasting more than 1 h. The many trials performed, and the analysis of fared data showed that only in very few cases this assumption does not hold. Therefore, in order to make a complete simulation of 1 h we need to assign two hours of demand, as represented in Figure 5.

The overall process is based on the assumption of maximum effectiveness of every subject: trains are always on time and all passengers take the reference time to walk from turnstiles to tracks and vice versa. This means that arrival times may be earlier than the actual ones.

In Figure 6 the program that calculates flow on edges and also the exiting passengers is presented. It is worth noting that we used Fared data (1 min aggregated and with OD information) only to build the average Percentage OD matrix (it gives the percentage of an origin going to a destination; the total by origin is 100%) because it is generally difficult to get this type of records, contrary to Turnstiled data (60 min aggregated) which in turn would be easily available. Differences between revealed turnstiled exit and assigned values per station are in average about 20%. This value can be partially explained by the difference in input and output data and by the use of a percentage OD matrix which refers to an average day.

Figure 7 shows the error between travel times indicated by data (Fared) and those calculated by our programs. If line transfers are included in the trip, the errors are almost Gaussian (with mean close to 0); if there are no line transfers, however, the errors are

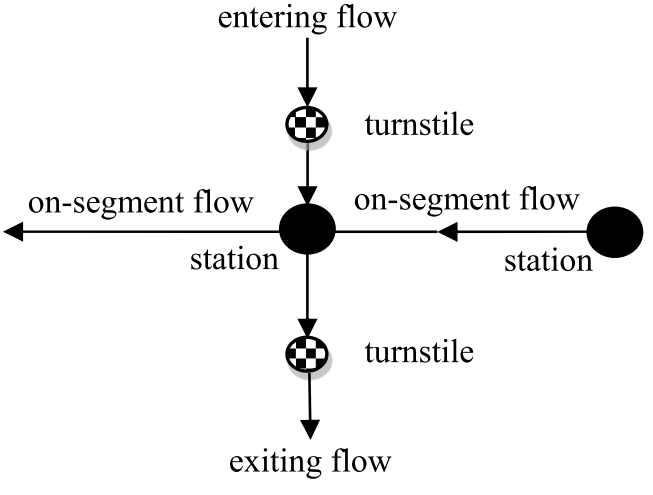

Figure 3. Schematic representation of passenger flows at a station node.

Starting steps - Creation of support datasets
list of stations with their attributes
percentage OD matrix by hour (from Fared data)
shortest time routes

REBO6: transforms data from a hourly basis to 1 and 10 minute basis

For each origin (Turnstiled data) and each minute

Distribution: Assign destinations (stochastic procedure)

Route selection: the shortest route to destination is selected from the archive

Train extraction: for each OD, the first useful train is extracted and travel time is calculated

Load of links: all links belonging to the shortest route are loaded and exiting flows of stations are updated

Figure 4. List of operations for the demand assignment.

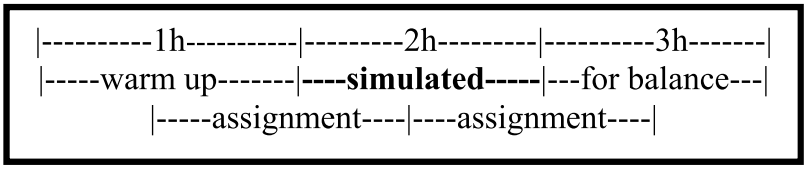

Figure 5. Warm-up, assignment, and balance intervals in the assignment procedure.

```
for each station
    calculate access time to track
    extract entry data from Turnstiled (1 hour aggregated)
    apply REBO6 programme to get 1 minute data
    select OD matrices for the two hours of assignment
    for each minute (1:120)
        distribute 1minute demand to destinations through a Monte Carlo routine
        for each destination
            calculate egress time
            extract the best route and the list of stations belonging to it
            for each route find the segments between stations
                calculate the earliest departure time
                find the first useful train
                calculate the travel time (and transfer times, if any)
                update the destination matrix (it is function of time)
                load each segment with the assigned demand (according to the travel time)
            end
        end
    end
end
```

Figure 6. Meta-language program of the edge loading procedure.

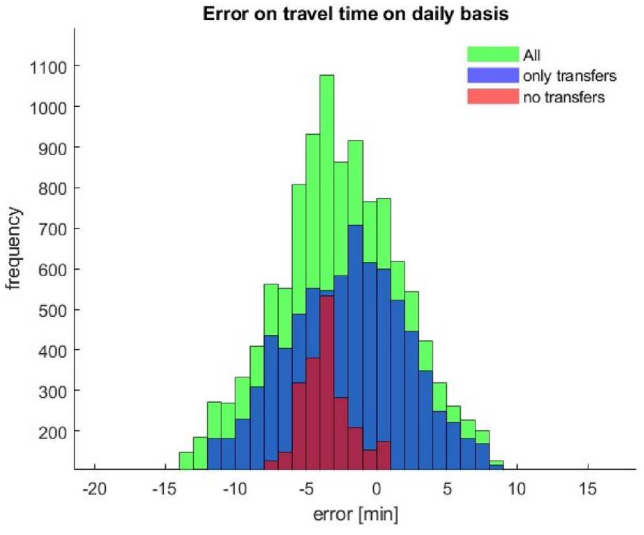

Figure 7. Error distribution between calculated and revealed travel times.

negative in the majority of cases (mode = −4 min) indicating that calculated duration is always overly optimistic.

3.5. The REBO6 programme

For each station and day of the week, the turnstiled data consists of 25 records: the first contains entries or egresses from 3:45am to 4:00am, the following 23 contain entries or egresses from x:00 to x:59, and the last one records entries or egresses from 3:00am to 3:45am. To fix ideas, we only consider entries in the following description. For egresses, the description is the same. The idea behind REBO6 is that entries every 10 min can be obtained from entries every 60 min as the result of three different processes: (a) 67.5% of the entries are uniformly distributed every 10 min; (b) 22.5% of the entries are allocated to the 10 min slots according to a random probability modelled according to the total number of entries during the hour before, the considered hour, and the hour next to the considered one; (c) 10% of the entries are allocated to the 10 min slots according to a completely random probability vector. To better explain the process in (b), let us call $Y(i–1)$, $Y(i)$, $Y(i+1)$ the number of entries at the hour before, at the hour of interest, and at the next one. If $Y(i-1) \leq Y(i) \leq Y(i+1)$, then we generate an increasing random probability vector. If $Y(i-1)\langle Y(i),\ Y(i)\rangle Y(i+1)$, then we generate a random probability vector increasing in the first half and decreasing in the second. If the inequalities are reversed, the order of the random probability vector changes accordingly. The chosen percentages have been selected so to have a good match with fared entries. For the first and last hours, we considered increasing and decreasing random probability vectors, respectively. To allocate at each minute the entries in 10 min, we use two different processes: (a) 70% of the entries are uniformly allocated at each minute; (b) 30% of the entries are randomly allocated. In this case, the percentages have also been chosen to have a good match with the fared data.

3.6. The centrality index Icentr

The centrality index Icentr was extensively discussed in a previous study (Mussone, Viseh, and Notari 2022), therefore, here we only mention its key features. It was created to evaluate the performance of transportation networks, taking into account both node weights and edge weights at the same time.

Definition of Icentr: it calculates the centrality index of each node by adding up the contributions of all edges in the graph, weighting them with a decrementing way in accordance with the order in which they are successively and continuously visited beginning at the node under consideration.

To describe how Icentr works, we consider an undirected simple graph $G = (V, E)$ that represents the network we take into consideration, and we assume that both nodes and edges are weighted. To fix notation, the nodes are $1, 2, \ldots, n$, and the edges are $e_1, e_2, \ldots, e_r$. Given an edge, each node in it is a neighbour of the other one. The notion of neighbour is at the core of the definition of Icentr. The weights of the nodes are $x_1, x_2, \ldots, x_n$ whereas the ones of the edges are $w_1, w_2, \ldots, w_r$, respectively. Let i_0 be the node we are calculating the index at. Firstly, we divide nodes and edges into levels, as follows. i_0 is the only level 0 node. The level 1 nodes are the neighbours of i_0, and they are $i_{11}, i_{12}, \ldots, i_{1n_1}$. The level 2 nodes are the neighbours of the level 1 nodes that are not in a previous level, and they are $i_{21}, i_{22}, \ldots, i_{2n_2}$. In general, a node is in level h if it is neighbour of a level $h-1$ node, and is not a neighbour of a node in level k for some $k < h-1$. Level h nodes are $i_{h1}, i_{h2}, \ldots, i_{hn_h}$. Because of the previous construction, no node belongs to two different levels and because the graph G is connected, every node belongs to a level. To divide edges in levels, we remark that an edge $e = \{i, j\}$ connects two nodes either in different levels, or in the same level. See in Figure 8 an example of how Icentr visits all edges.

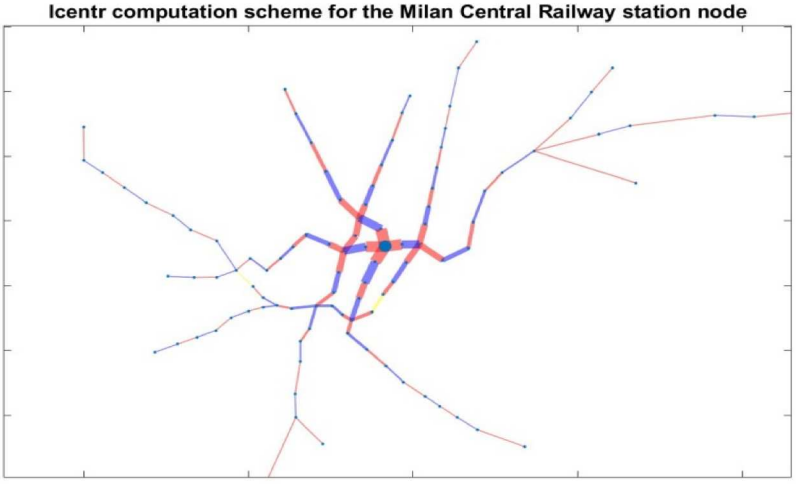

Figure 8. The scheme followed by Icentr to visit the whole graph; in the example, the starting node is the Central Railway Station node (the blue circle); blue and red colours identify the consecutive steps of visiting edges; the yellow colour identifies edges visited by two directions at the same time.

This choice of levels for the edges corresponds to the order in which they can appear in a path starting from i_0. If e connects two nodes at different levels, let $x(e)$ be the weight of the node at the maximum level in e. Then, the contribution of e to the value Icentr takes at i_0 is

$$ic(e) = \frac{x(e)}{2^{lev(e)-1}}\, w(e) \tag{1}$$

If $e = \{i, j\}$ connects two nodes at the same level whose weights are x_i, x_j, respectively, the contribution of e to the value Icentr takes at i_0 is then

$$ic(e) = \frac{x_i + x_j}{2^{lev(e)}}\, w(e) \tag{2}$$

The final value of the index is simply the sum of the partial contributions, and so we have

$$Icentr(i_0) = \sum_{j=1}^{r} ic(e_j) \tag{3}$$

If we assume that every node and every edge have weight 1, a node has a higher ranking if the edges of the graph are closer to the node, according to the levels we construct to explore the graph starting from the given node. The partition of nodes in levels looks similar to that needed to construct a spanning tree, rooted at i_0. In addition, in the computation of Icentr, we consider all edges in the connected component containing the node i_0.

The outcomes can be reported numerically in a text file or by using the graph (see for example Figures 11 and 17 in the section 4) where the circles representing the nodes have either different size or different colour or both, according to their index value.

3.7. The image processing application

As previously said, outcomes of index calculation can be successfully presented by a graphical representation based on the same graph layout. The index value of each node can be shown either by using different colours or by varying the size of a node (generally represented by a circle). In other words, graphs reporting centrality index values of nodes are, in the end, images coded by a RGB map. Each pixel of the map (that carries a single value) is represented by a triplet of numbers ranging from 0 to 255 (according to the related colour). The combination of these three numbers determines the pixel colour. As a result, the radius and colour of the circles on the graph can be used to determine their centrality index values.

Hence, those images can be the object of math operations: sum, difference, division, multiplication and so on. Interpretation of the outcomes of these operations may be simply to find how the resulting image is coloured or to calculate distances between two images. In the latter case, if an increasing scale of colours (the index range [0,1] has to be multiplied by 255) is selected, the change in colour corresponds to a proportional change in value (Figure 9). The same outcome can be achieved by increasing the area associated to the object representing the current scenario (Figure 10).

Since white colour is [1, 1, 1] and black is [0, 0, 0] and generally background of images is white, operations must be carried out using the complement to 255 of triplets.

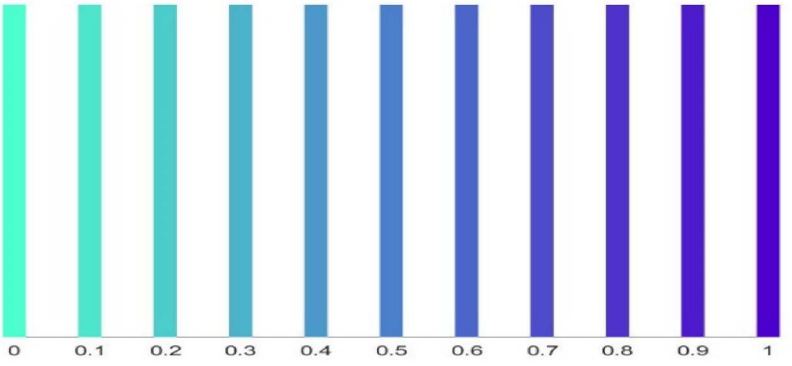

Figure 9. Colours obtained for the increasing scale of x from 0 to 1 (0–255) of colours of the basic triplet [0.3, *x*, 0.8].

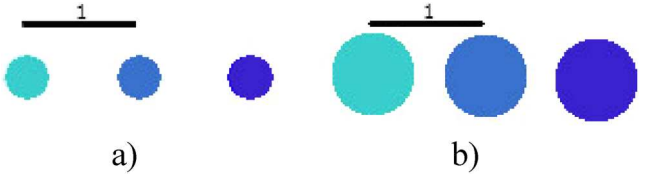

Figure 10. Examples of objects of different colour ($x = 0, 0.5, 1$) and size; the circles in (b) have a radius double of that in (a).

In Figure 9 an example of consecutive colours for the triplet [0.3, x, 0.8] where x goes from 0 to 1 is reported. In Figure 10 two different cases are considered by changing the colour and area of the circles. In Figure 10(a), the difference between the circles is 0.5*A (from left to right, and A is the area of the circles), in Figure 10(b) is 4*0.5*A.

The method can be applied to every circle by changing simply their colour and/or by increasing the size of coloured objects which further amplifies differences. However, resizing must be done with caution due to the possibility of object overlap, which could be a source of distortion.

The suggested method converts the topological evaluation of centrality index values into an image evaluation. It is not a bijective operation since different patterns resulting from various topologies can provide the same outcomes. Actually, given a topology, other object colours can also produce the same outcomes. As a result, rather than doing an absolute evaluation, the procedure may be more suited for case comparison, and comparison between images referring to consecutive instants or with a reference case can be considered appropriate.

4. Results and discussion

4.1. Dynamics of passenger flows

Before analysing the dynamics of centrality indices, we analyse the dynamics of passenger flows.

The assignment procedure, described in section 3.3, allows us to examine all the outcomes of the simulation. The way outcomes are presented is threefold: numerically, through tables and statistics, graphically and through image processing. The latter two instances allow us an even higher synthesis.

For the graphical side: firstly, a synoptic graphic displays three subplots, each of which contains the Milan graph showing the flow on the edges, the entering flow, and the exiting flow by node. The outcomes can be produced at intervals of one to sixty minutes, and consequently the synoptic graphics are updated (Figure 11 proposes an example of two consecutive frames at one minute). Secondly, graphics depict the change in segment load with time (Figure 12 displays dynamics for the top five loaded

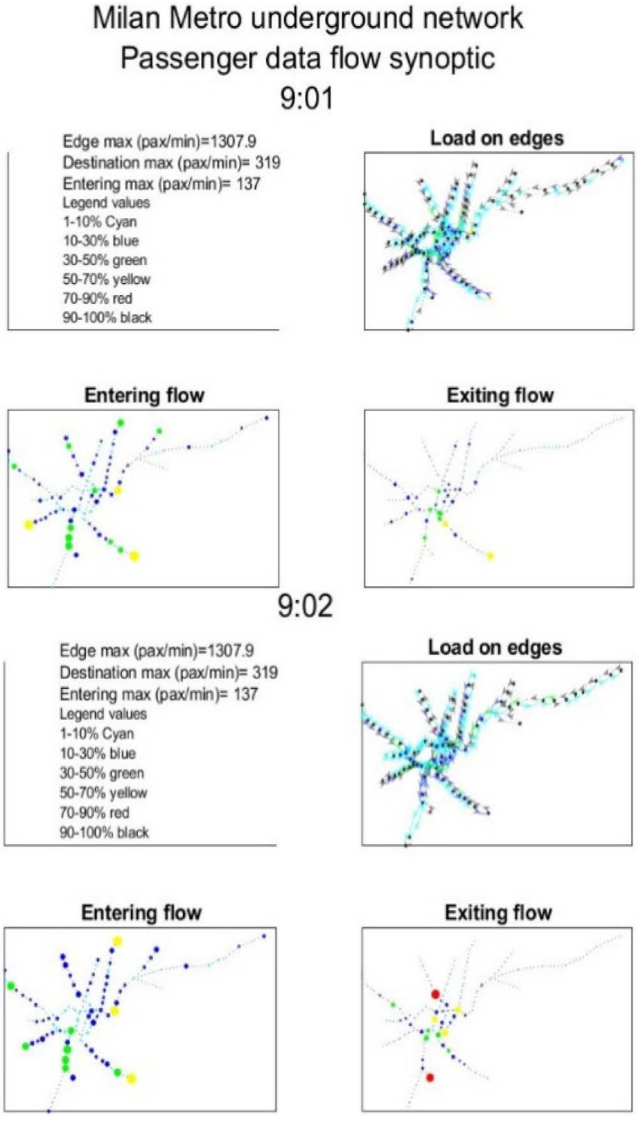

Figure 11. Synoptic view of flow analysis by minute, at time 9:01 and 9:02.

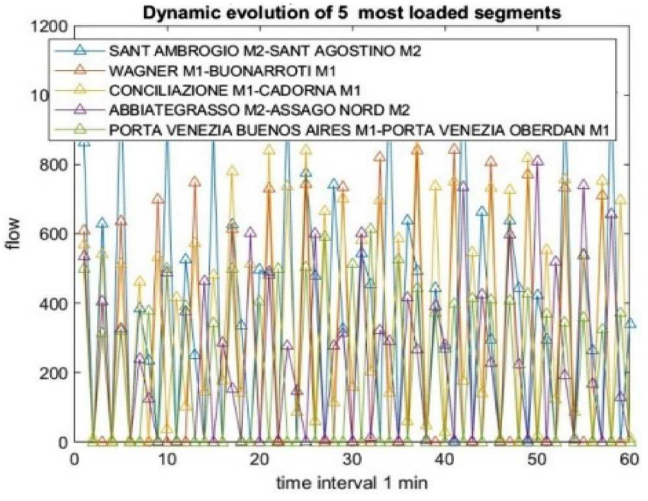

Figure 12. Most five loaded segments from 9:00 to 10:00 am.

segments), departing flows (Figure 13 depicts dynamics for the top five exiting stations), and finally, entering flows (Figure 14 shows dynamics for the most five entering stations). Thirdly, a 3D figure (Figure 15) displays the load for each section for the left and right ways of circulation throughout the course of an hour.

Even though Figure 11 just represents the beginning of a sequence, it is clear that there are significant changes between the graphics for 9:01 and those for 9:02, and actually, these differences characterize all the sequence. Then, this type of representation is appropriate to visually analyse the overall process. It is worth noting that the normalization values used to size and colour the circles of nodes are different between the three graphics and, therefore, the plots can be compared only between subplots of the same subject.

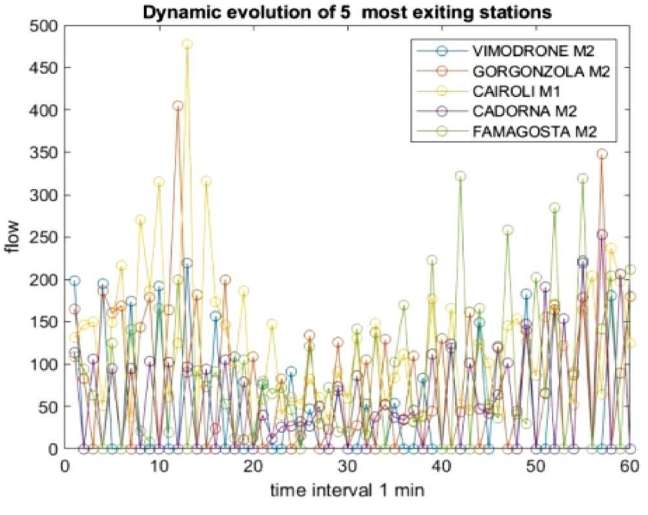

Figure 13. Most five exiting stations from 9:00 to 10:00 am.

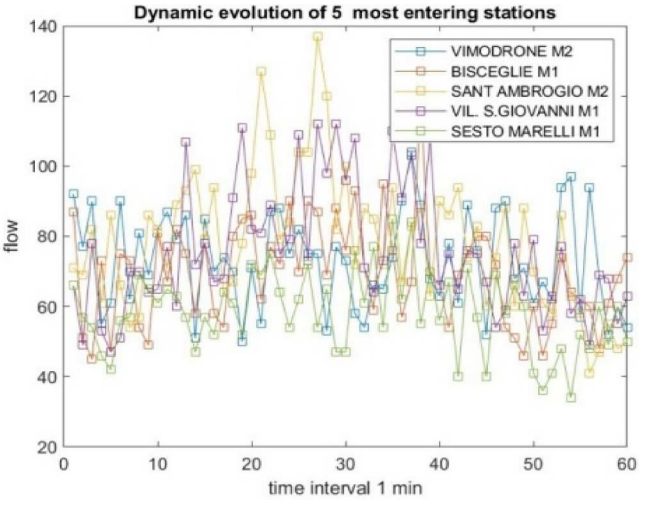

Figure 14. Most five entering stations from 9:00 to 10:00 am.

In Figures 12–14, the scales of the y-axis gradually get smaller by a factor of around 3 from segment load to exiting flow to incoming flow. This asserts that, depending on the station and the time the data correspond to, the three processes are controlled by different mechanisms. Segment loads are influenced by train frequency; exiting flows are influenced by the system activity, and entering flows are influenced by residence, or vice versa, depending on whether a movement is outward or return. This reflects also in the shapes of the curves: in Figure 13 (for exiting flows) they have sharp peaks, whereas in Figure 14 (for entering flows) they exhibit subtle oscillations around an average value.

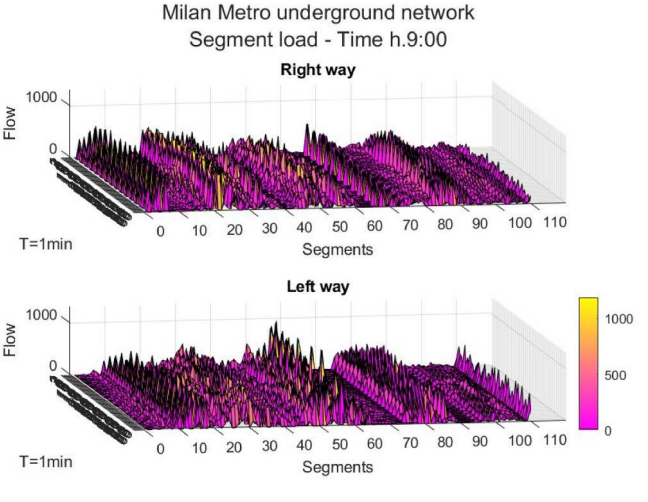

Figure 15. Flows over one hour by steps of one minute on the two ways of the segments from 9:00 to 10:00 am.

Figure 15 reports the 110 segment loads per 1 min interval and by direction of travel. Actually, the direction is clear for segments belonging to legs connecting to terminals: the right way is from terminal to the centre, and the left way is the reversed; for central segments, it depends on how the segment is coded. In any case, it is clear that the two representations are nearly complementary to one another.

4.2. Image comparison of passenger flow data

The images showing the passenger flows (by load on edges, entering in stations, and exiting) are processed according to the above-mentioned procedure of image processing (Section 3.5). Two consecutive images at instants t and $t + \mathrm{T}$ are processed at a time as part of the series of images created at a given aggregation time. So, if the aggregation time, T, is 5 min, in an hour there are 11 pairs of images to be processed. The comparison is performed by simply taking the absolute and arithmetic difference between the two images. The absolute difference accounts for changes in whichever direction they occurred, and, therefore, measures the total variability between images; if it increases, it means that differences are increasing. The arithmetic difference accounts for everything that is not compensated between images; the outcome could be null due to the fact that the two images are equal or there are points in the first image with higher values than in the second one and contemporary there are points in the second image with higher values than in the first. Results are positive when the previous image (at instant t) has higher value points, conversely, are negative when the following image (at instant $t + T$) has higher value points. The two outcomes (absolute and arithmetic differences) are equal when all the differences are positive or negative, in this case except for the sign. The arithmetic difference oscillates around zero when there is an alternation between the values of images.

In Figure 16 the two types of outcomes are reported for each image comparison (calculated for load on segments, entering and exiting flows) for three aggregation times, 1, 5, and 10 min and for hours 9:00 and 8:00.

It is worth noting that these analyses concern differences and not values of a single image, therefore no information can be deducted about the real quantities at play. As it would be expected, the aggregation interval serves as a low-pass filter. The 5-minute break appears to be a reasonable balance between representational details and computational cost. Figure 16's curve analysis for 9:00 reveals the following:

(1) Load on segments (red and black curves), the absolute differences (represented by red curves) have a maximum at about 9:30 and arithmetic differences (represented by black curves) oscillate but with the mean that becomes more negative, meaning that the differences between images increase until 9:30 and after that they decrease, and load is becoming progressively higher at t + T;
(2) The entering curves (blue and cyan curves) have a significant positive peak at about 9:30, indicating a strong reduction of entering flow;
(3) The exiting curves (green and yellow curves) are the most smoothed curves, generally in counter-phase with load curves, meaning that exiting values do not change

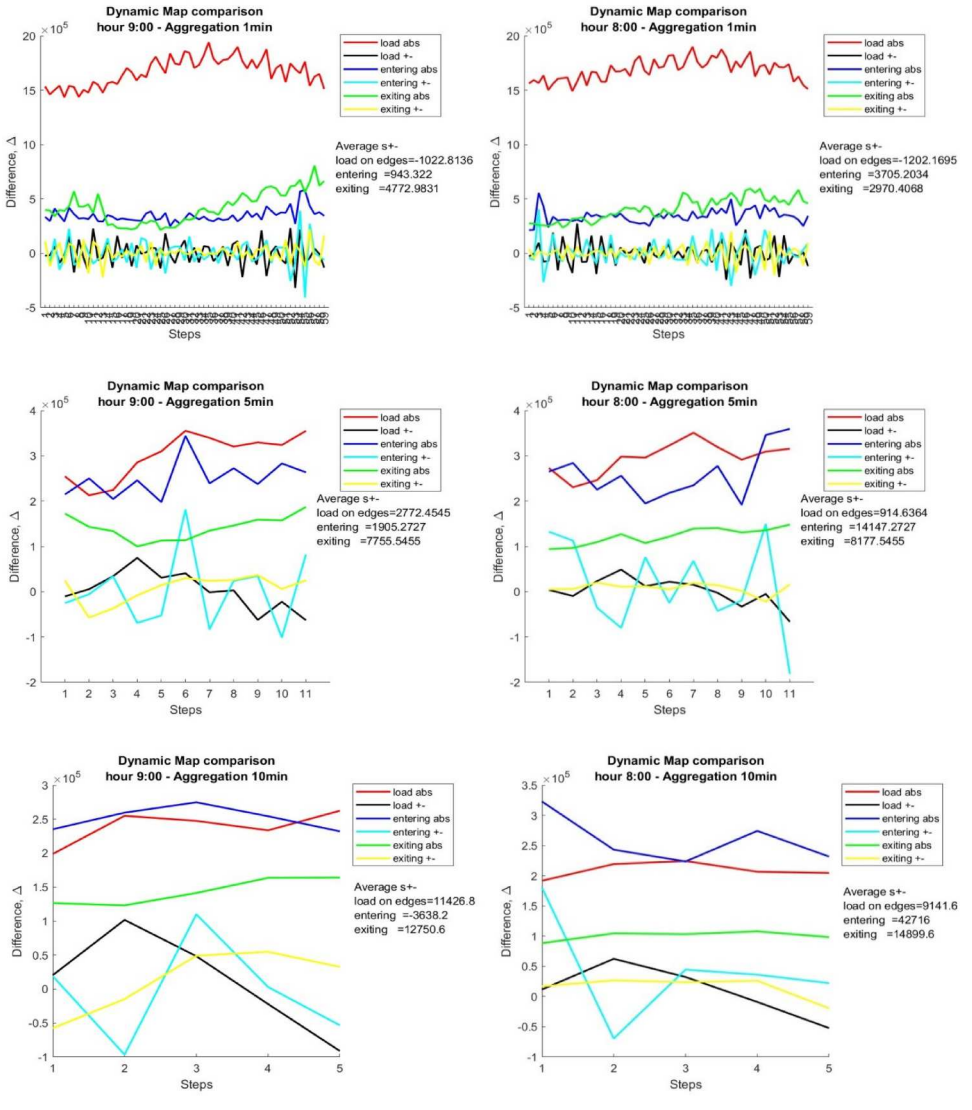

Figure 16. Comparison of image processing outcome applied to passenger data for hour 9:00 (left) and 8:00 (right) and four aggregation times (1, 2, 5, and 10 min).

much over the hour; it is observed an increase of absolute differences for exiting curves and the average value for the arithmetic differences is positive, meaning that exiting flow is progressively becoming smaller;

(4) The differences for load absolute curves are significantly greater than for entering and exiting curves, the lower the aggregation time, T, is, meaning that values at play are higher for load segment flows;

(5) There is not a significant difference between outcomes computed for 8:00 and 9:00 (Figure 16), whereas relevant differences are present in outcomes of the evening hours (e.g. for 19:00).

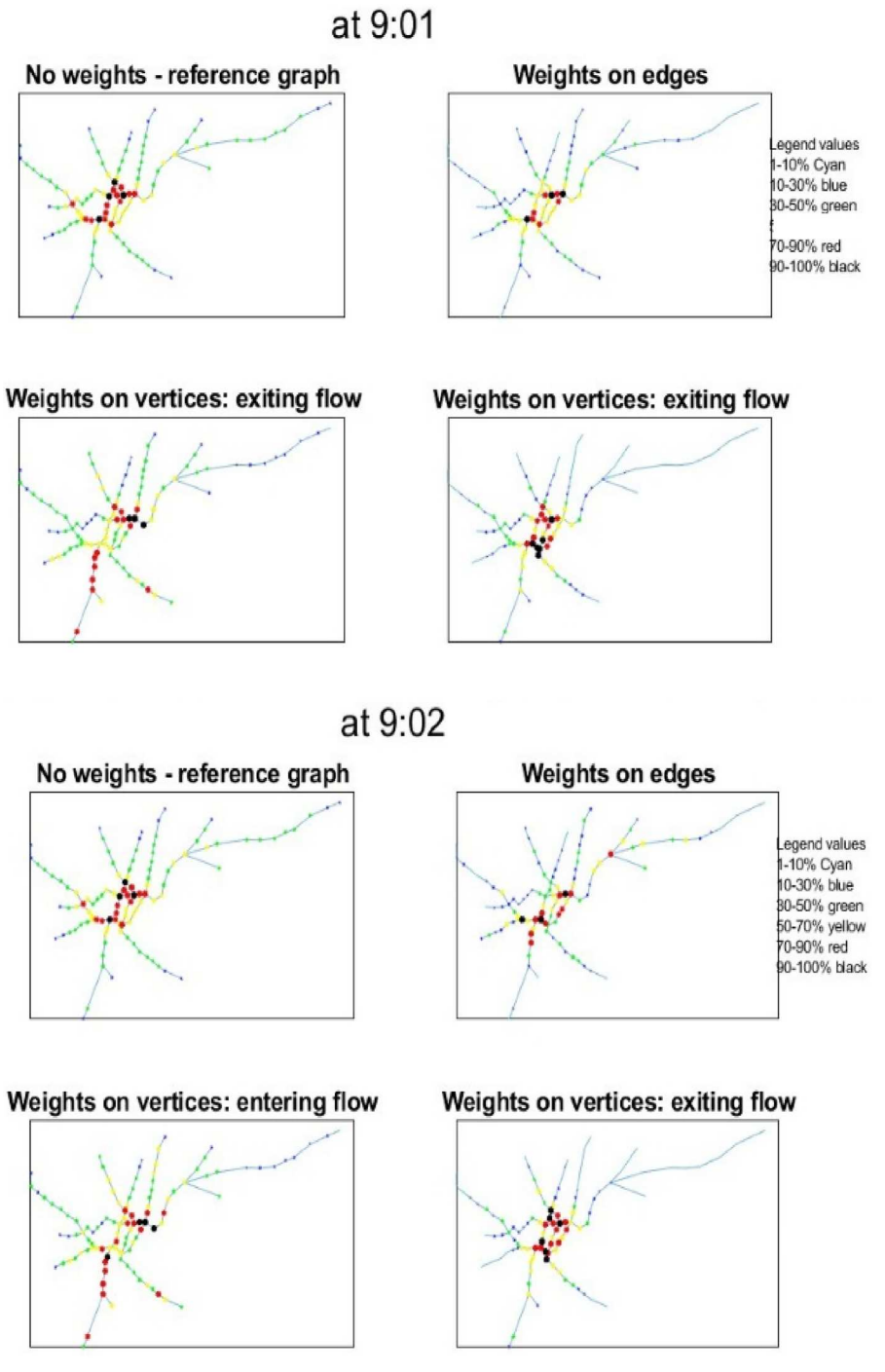

Figure 17. Synoptic view example for centrality index change analysis by minute at time 9.01 and 9:02.

4.3. Dynamics of Icentr centrality index

The Icentr program calculates the index values using the passenger flows (previously calculated as in section 3.3) as weights for the edges (by using the segment load) or the nodes (by using the entering or exiting flow) of the graph. Icentr is calculated for every instant (at the aggregation time, T) in the considered hour, and this allows us to see how indices change over time. Then, information given are different from that achieved by the 'simple' analysis of passenger flow dynamics developed in section 4.1.

Firstly, the outcomes are presented in a graphic with four subplots, representing the following: the indices for the graph without flow weights, with load flow on the edges, the entering and the exiting flow on the node. At each time step, T, the synoptic graph is updated.

In Figure 17, two consecutive examples of calculation for $T = 1$ min, starting from 9:01 am, are shown. The first subplot is fixed (no weights are applied) and can be used as a reference scenario for the other subplots. The other subplots show, notwithstanding the closeness in time, clear differences especially for the weights on edges (top right). From each subplot of this figure, it is possible to see what stations and segments are more relevant (for example, looking at stations with the black colour). From the comparison of the plot for times 9:01 and 9:02, we can see how rapidly the set of relevant stations changes. This high dynamic range is represented in the rough synthesis of Figure 18.

In the same Figure 18, the effect on nodes representing the most 5 stations for the considered type of flow at 9:00 am and aggregation times equal to 1 and 10 min is shown using the three weight strategies. Note that the y-axis scale is different for 1 and 10-minute aggregation times, T, and for the three types of flow. However, the shape of points remains the same by changing T, except for the absence of oscillations in the graphics with $T = 10$ min. For the cases of weights on segments and on nodes with entering flows, the index values follow a convex curve shape whereas for weights on nodes with exiting flows, the shape is concave. This demonstrates the reverse relationship between on-segment and entering flows and exiting flows: as entering flows increase, the exiting flows decrease. The most valued stations are similar for on segment and entering flows, but completely different from those for exiting flows. This emphasizes the counter-phase behaviour of entering and exiting flows with a shift of about 30 min, which could be just the average journey duration.

Figure 19 shows the Icentr values for all the 107 stations for the hour of 9:00 and for 1 (a) and 10 (b) minute aggregation times, T. It is simple to spot the four ridges, which are mostly made up of stations on the same subway line. The first ridge is for station 24 (Duomo, line M1), the second for station 49 (Garibaldi Railway station, line M2), the third for station 80 (Montenapoleone, line M3), and the fourth for station 99 (Isola, line M5).

Their overall shape does not change much with T, but the y-scale does and naturally, many significant peaks disappear when $T = 10$.

In this view, T has a clear effect on the index, implying the usage of short time intervals to find meaningful peaks. Aside from that, a comparison of Figure 19(a,b) shows that the longer the aggregate period, the smoother the index values by station. Actually, altering T allows the station on the crest to change, but only in respect to the stations nearest to it and on the same line.

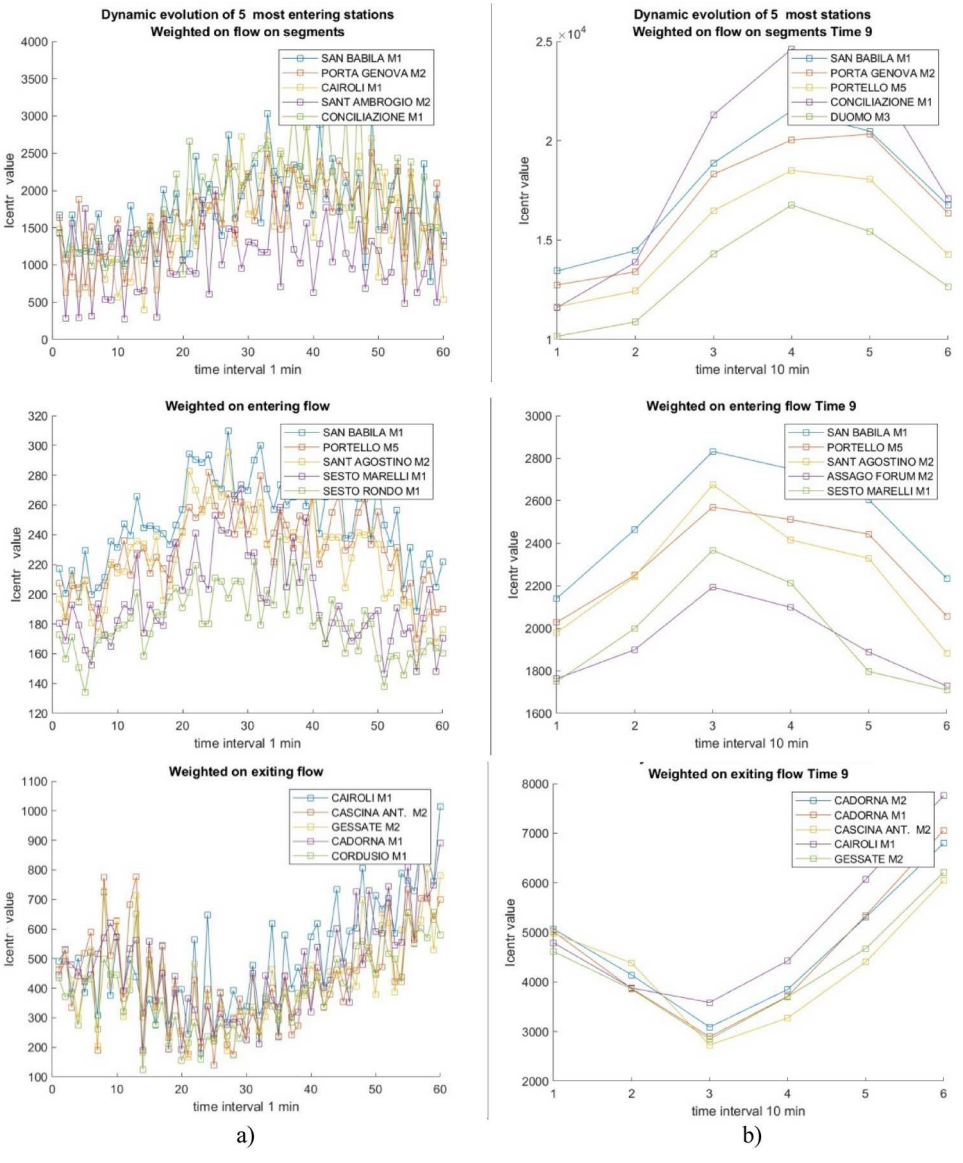

Figure 18. Top 5 stations for Icentr with aggregation of 1 and ten minutes for hour 9:00 with the three weighting strategies.

This is a qualitative analysis because we are primarily interested in describing the procedure, but a quantitative approach may clearly be used to analyse the relevance of peak values.

4.4. Image comparison of Icentr values

Also, in the case of the analysis of Icentr values, two different outputs are given for image analysis of synoptic graphics: the absolute, d1 (called abs.), and arithmetic, d2 (called +–),

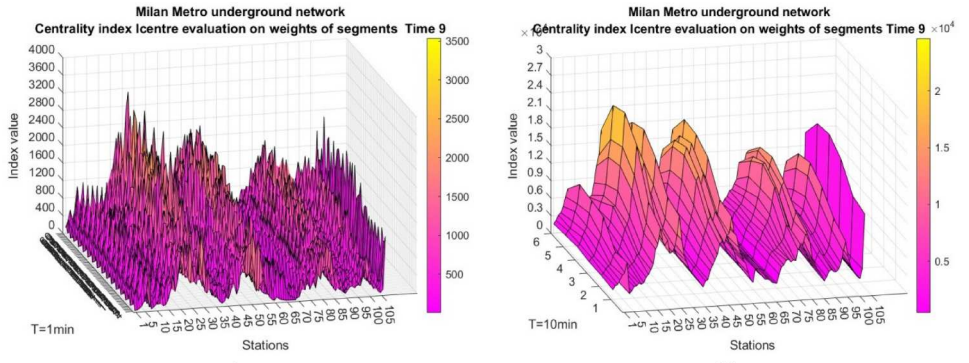

Figure 19. Icentr values for all stations for hour 9:00 with aggregation of 1 (a) and 10 (b) minutes by using the load on segment flows as weights for edges.

values, as already done in section 4.2; the descriptions and comments about their meanings hold here as well.

If arithmetic difference, d2, is positive, it means that in most cases the old value is greater than the new one, and vice versa it happens for negative values. If d1 is constant, it means that the index values oscillate at the same values.

The following four cases can be taken into consideration by combining the two outputs:

(1) d1 increases and d2 > 0: differences are becoming larger because new values are progressively decreasing;
(2) d1 decreases and d2 > 0: differences are becoming smaller because new values are progressively decreasing;
(3) d1 increases and d2 < 0: differences are becoming larger because new values are progressively increasing;
(4) d1 decreases and d2 < 0: differences are becoming smaller because new values are progressively increasing.

The images displaying the Icentr values (for load on edges, for flow entering and exiting stations, used as weights) are processed in the manner described above, producing two curves for each weight type: the absolute (d1) and the arithmetic (d2) difference between two consecutive images for three aggregation times, 1, 5, and 10 min.

In Figure 20, the two types of curves are reported for the hours 9:00 and 8:00; it is worth mentioning that the number of points on the x-axis is given by $[(60//T) - 1]$ (where T is the aggregation time) because a point represents a difference of values at two consecutive times. These figures appear visibly different from those carried out for passenger flow data (Figure 16). The oscillations of values are many more and only for the 10-minute interval the curves become smooth. The differences between the hours of 9:00 and 8:00 are much more evident than those seen when analysing the passenger flow data. This has to do with the use of Icentr which amplifies oscillations present in raw data over time. The curves for entering and exiting flow weights (blue and cyan, green, and yellow, respectively) are neither synchronized between them nor with the on-segment

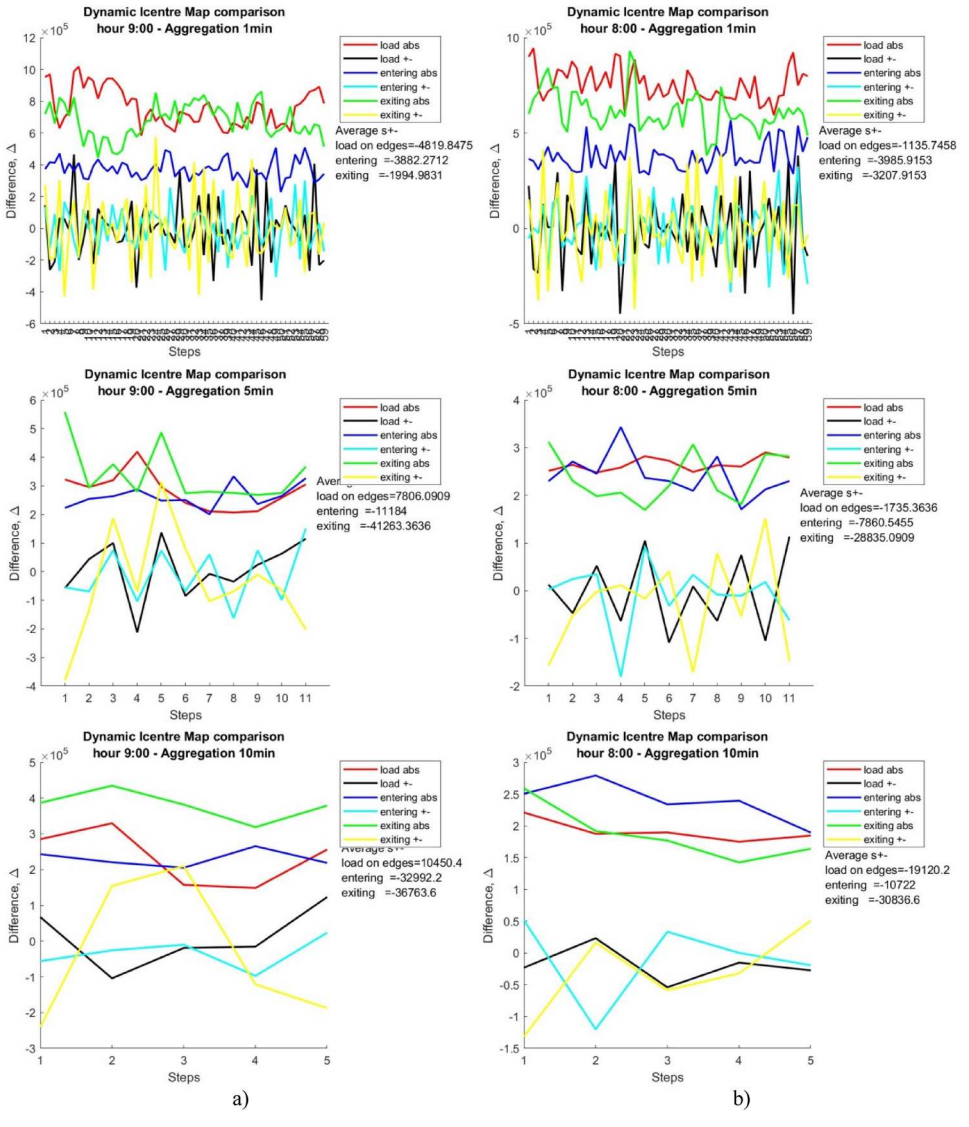

Figure 20. Comparison of image processing outcome applied to Icentr values weighted by passenger data for hours 9:00 (left) and 8:00 (right) and three aggregation time (1, 5, and 10 min); d1 = abs. curves, d2 = arithmetic curves.

load weight curve; actually, all three curves are phase shifted, but the on segment and exiting flow weights are a little bit more on phase. Also in these figures, the entering flow weight curves for d2 are the most smoothed, but the related d1 curves still oscillate significantly. This implies that variations in rough data do affect Icentr values, but the values cyclically vary on the same numbers (then the absolute difference does not change).

Also, $T = 5$ min appears to be a good compromise between details and computing burden in these figures, but the peaks in the 1-minute representations (not reproduced in the 5-minute figures) may be significant when compared to some reference thresholds (such as those related to train capacity or passenger flow facilities).

For $T = 10$ min, the analysis is easier (because of the small number of points). Consider Figure 20(a) with just $T = 10$ min. Starting with d2 curves, we can say that at the first step, the index for entering (cyan curve) is negative (entry is increasing), but the index for exiting (yellow curve) is more negative (it is increasing much more), causing the index of the loading (black curve) to be positive, indicating that loading is decreasing. In the following step the situation changes because exiting becomes positive, entering is almost nil, then the loading curve becomes negative, that is, loading increases. From d1 curves instead we can argue how numerous and relevant are the changes (for example, due to the moving of the train from a station to the following one). A similar analysis can be performed for the remaining steps and other T.

The comparison of the results for the hours 9:00 and 8:00 reveals dramatically distinct curves, showing that they correspond to different processes. The only similarity is the presence of numerous oscillations for all three types of curves.

The advantage of these studies is that they give us quick information on what's happening in the network, such as whether or not there are changes between the state at instant t and the state at instant $t + T$ (where T is the aggregation step) and if so, in what direction. The problem is that we don't know how big of an area is impacted by the change or where the changes are occurring (if any). Future studies will be conducted on this task.

When compared to the current literature, the proposed study is more than a least common multiple of research on the topic of dynamic analysis of underground networks.

One essential element is that this type of study must consider the entire network rather than just a single line due to the numerous interactions between lines. It overtakes the issue of assuming a constant train speed by using timetables (of course, when studying the effect of failures or performance reductions, this assumption must be eliminated). The results suggest that the three categories of passenger flows (entering, exiting, and on segment) have distinct dynamics that should be investigated jointly. The origin/destination model of passenger demand is critical for the successful assignment of passenger flow and so demands special attention. The introduction of centrality indices is another significant addition of the suggested method. In particular, the novel index Icentr has a high ability to identify emerging stations as the most important, as opposed to raw passenger data. Furthermore, time discretization is important since large changes in indicators are detected in the one-minute study.

Finally, dealing with such a large number of outcomes necessitates the use of specific methodologies to provide synthesis. Image processing provided useful insights in this regard, and image classification using deep learning technologies could provide much more.

5. Conclusions

The methodology for identifying stations in an underground network for which the impacts of a disruption would be more relevant is proposed in this study. Because of its nature, the work is interdisciplinary, requiring understanding of subjects other than transportation, such as simulation software, image analysis, and graph theory. Contribution to transportation planning is primarily concerned with the knowledge of train load factor over each segment per time interval (with a minimum of one minute), followed by train schedule improvements.

We focused on underground networks because this type of transport allows us to get all the information about passenger flows, but there are no limitations on applying it to other transport systems. Yet, the application to the case of Milan has the same explanation related to the availability of data. Of course, the pre-processing of data could change according to their format. The methodology is based on a dynamic approach that takes into account the change in demand (ridership) over time, with a time resolution of 1–30 min. Specific programmes were implemented to simulate the assignment process and retrieve the three components of demand: entering and exiting the stations, and segment (the line between two consecutive stations) load, that are used to dynamically interact with the graph of the network by weighting its nodes and edges.

We employed the Icentr centrality index (proposed in the earlier works by Mussone, Viseh, and Notari 2020; 2022), which is particularly appropriate for this application because it enables us to take into consideration weights on both nodes and edges of a graph. Yet, it is not particularly demanding on the computing burden for large networks and therefore can be successfully applied to the many calculations required when a short aggregation time is adopted.

It is worth noting that for the type of analysis, required evaluation approaches such as the use of statistical indicators (like mean or variance) are not particularly suitable because, by their nature, they tend to filter out singular phenomena (like, for example, a peak of passengers), which instead are crucial for our purposes and therefore must be revealed.

For the purpose of synthesizing the generated outcomes, a programme based on image processing methods was developed.

The analysis has been firstly focused on the raw data of passenger flows and then on the application of a centrality index in order to evaluate how network performance changes over time when passenger flows (that change over time) are used as conditioning weights. The use of centrality indices allows such an evaluation, taking into account the network topology and its other specific features; the use of passenger flows allows us to measure the importance of edges and stations. The higher the flow, the more 'important' the station or the segment.

The effects of passenger flows in an underground network were performed at different aggregation times. Each of them gives different information, though they are correlated. Therefore, it is critical to understand what it means to assume a certain time for data aggregation. The paper also faces this issue by analysing the structure and time evolution of passenger flows, both entering and exiting the stations, and those representing the load on segments. We observed a great deal of variability in passenger statistics, especially at 1-minute interval aggregation times. This is expected for the exiting flow, which depends on train scheduling, i.e. when the train arrives at the station, passengers can exit; it is also expected for segment load flows, which depend on segment length, train headways, and entering and exiting flows. It is somewhat unexpected for the entering flows for which it is expected a smooth arrival curve; but, it is worth noting that their values are determined by a semi-random procedure called REBO6 that takes as input entering flows aggregated by 1 h (see Section 3.2) and outputs them at 1-minute interval simulating the actual dynamics of entering flows as recorded in the 'Fared' data. This variability is amplified when calculating the centrality indices after flows are applied as weights. The use of a centrality index makes the effects of passenger flow on the network clearer.

The three passenger flows (entrance, exit, and on-segment) constitute distinct processes, particularly in terms of their dynamics, and the proposed approach exhibited the capacity to assess them.

We created the programs to manage data at the highest possible resolution. Some values of time, such as those in schedules or transfer times, have a precision of 1 s, whereas others have a resolution of 1 min. The results were then combined at intervals of 1 to 2, 5, 10, 15, 20, and 30 min. They differ in how they rank stations (for entering and exiting flows as well as for on-segment flow), which raises the question of why and how to select one.

Implications for planning concern mainly the use of the overall methodology to simulate and, then, to study how, by changing the train's scheduled service, the train passenger load changes. This has two fallouts: first, the passenger flow at stations and platforms can be controlled and dimensioned opportunely; second, the relevance of stations (according to the proposed centrality index) can be distributed homogeneously among stations avoiding or mitigating critical concentrations only in a few stations.

Future research will address:

- Improving the assignment procedure with other models to create the percentage OD matrix;
- Calculating the load by train as well;
- Using other centrality indices to further investigate the topology effects;
- Considering the train schedule times and the passenger times (from turnstile to the platform and vice versa, and transfer times) stochastic;
- Clustering areas on the network with the highest sum of index values to understand whether the effects are local and isolated or involve a wider area than a single station.

Acknowledgements

Thanks are due to AMAT-MI Agency of Milan Municipality (Italy) for providing data for this research.

Disclosure statement

No potential conflict of interest was reported by the author(s).

References

Ait-Ali, A., and J. Elíasson. 2019. "Dynamic Origin-Destination Estimation Using Smart Card Data: An Entropy Maximisation Approach." 1–15, arXiv: Optimization and Control.

Alvarez-Socorro, A., G. Herrera-Almarza, and L. González-Díaz. 2015. "Eigencentrality Based on Dissimilarity Measures Reveals Central Nodes in Complex Networks." *Scientific Reports* 5:17095. https://doi.org/10.1038/srep17095.

Barthelemy, M. 2004. "Betweenness Centrality in Large Complex Networks." *The European Physical Journal B* 38 (2): 163–168. https://doi.org/10.1140/epjb/e2004-00111-4.

Cheng, Y.-Y., R. K.-W. Lee, E.-P. Lim, and F. Zhu. 2015. "Measuring Centralities for Transportation Networks Beyond Structures." In *Applications of Social Media and Social Network Analysis*, edited by P. Kazienko and N. Chawla, 23–39. Cham: Springer. https://doi.

org/10.1007/978-3-319-19003-7_2. https://ink.library.smu.edu.sg/cgi/viewcontent.cgi?article=4642&context=sis_research.
Chiang, L.-Y., R. C. Crockett, I. C. Johnson, and A. O'keefe. 2017. *Passenger Flow in the Tube*. E-Project-062317-051103. London: Worcester Polytechnic Institute.
Chopra, S. S., T. Dillon, M. M. Bilec, and V. Khanna. 2016. "A Network-Based Framework for Assessing Infrastructure Resilience: A Case Study of the London Metro System." *Journal of the Royal Society Interface* 13 (118): 20160113. https://doi.org/10.1098/rsif.2016.0113.
Cui, A. 2006. "Bus Passenger Origin-Destination Matrix Estimation Using Automated Data Collection Systems." Massachusetts Institute of Technology. http://hdl.handle.net/1721.1/37970.
Derrible, S. 2012. "Network Centrality of Metro Systems." *PLoS One* 7 (7): e40575. https://doi.org/10.1371/journal.pone.0040575.
Derrible, S., and C. Kennedy. 2010. "The Complexity and Robustness of Metro Networks." *Physica A: Statistical Mechanics and Its Applications* 389 (17): 3678–3691. https://doi.org/10.1016/j.physa.2010.04.008.
Derrible, S., and C. Kennedy. 2011. "Applications of Graph Theory and Network Science to Transit Network Design." *Transport Reviews* 31 (4): 495–519. https://doi.org/10.1080/01441647.2010.543709.
Dimitrov, S. D., and A. Ceder. 2016. "A Method of Examining the Structure and Topological Properties of Public-Transport Networks." *Physica A: Statistical Mechanics and Its Applications* 451:373–387. https://doi.org/10.1016/j.physa.2016.01.060.
Freeman, L. C. 1978. "Centrality in Social Networks: Conceptual Clarification." *Social Networks* 1 (3): 215–239. https://doi.org/10.1016/0378-8733(78)90021-7.
Gu, Y., X. Fu, Z. Liu, X. Xu, and A. Chen. 2020. "Performance of Transportation Network Under Perturbations: Reliability, Vulnerability, and Resilience." *Transportation Research Part E: Logistics and Transportation Review* 133:101809. https://doi.org/10.1016/j.tre.2019.11.003.
Guo, W., and X. Lu. 2016. "London Underground: Neighbourhood Centrality and Relation to Urban Geography." 2016 IEEE International Smart Cities Conference (ISC2), Trento, Italy.
Hong, L., W. Li, and W. Zhu. 2017. "Assigning Passenger Flows on a Metro Network Based on Automatic Fare Collection Data and Timetable." *Discrete Dynamics in Nature and Society* 2017:4373871, 10 pages. https://doi.org/10.1155/2017/4373871.
Hu, Y., F. Chen, P. Chen, and Y. Tan. 2017. "The Influence of Passenger Flow on the Topology Characteristics of Urban Rail Transit Networks." *International Journal of Modern Physics B* 31 (12): 1750181 (18 pages). https://doi.org/10.1142/S0217979217501818.
Jiang, B., and C. Claramunt. 2016. "Topological Analysis of Urban Street Networks." *Environment and Planning B: Urban Analytics and City Science* 31 (1): 151–162. https://doi.org/10.1068/B306.
Kuhlman, W. 2015. "The Construction of Purpose Specific OD Matrices Using Public Transport Smart Card Data." 149. http://repository.tudelft.nl.
Kumar, A., K. Haque, S. Mishra, and M. M. Golias. 2019. "Multi-Criteria Based Approach to Identify Critical Links in a Transportation Network." *Case Studies on Transport Policy* 7 (3): 519–530. https://doi.org/10.1016/j.cstp.2019.07.006.
Lam, W. H. K., Z. X. Wu, and K. S. Chan. 2003. "Estimation of Transit Origin–Destination Matrices from Passenger Counts Using a Frequency-Based Approach." *Journal of Mathematical Modelling and Algorithms* 2 (4): 329–348. https://doi.org/10.1023/B:JMMA.0000020423.93104.14B.
Latora, V., and M. Marchiori. 2002. "Is the Boston Subway a Small Worlds Network?" *Physica A: Statistical Mechanics and Its Applications* 314 (1–4): 109–113. https://doi.org/10.1016/S0378-4371(02)01089-0.
Liu, J., and X. Chen. 2019. "Simulation of Passenger Motion in Metro Stations During Rush Hours Based on Video Analysis." *Automation in Construction* 107:102938. https://doi.org/10.1016/j.autcon.2019.102938.
Loukaitou-Sideris, A., B. D. Taylor, and C. Turley. 2015. *Passenger Flows in Underground Railway Stations and Platforms*. Mineta Transportation Institute Final Report No. MTI 12-43, 110 pp.
M'Cleod, L., R. Vecsler, Y. Shi, E. Levitskaya, S. Kulkarni, S. Malinchik, and S. Sobolevsky. 2017. "Vulnerability of Transportation Networks: The New York City Subway System Under

Simultaneous Disruptive Events." *Procedia Computer Science* 119:42–50. https://doi.org/10.1016/j.procs.2017.11.158.

Mohammed, M., and J. Oke. 2023. "Origin-Destination Inference in Public Transportation Systems: A Comprehensive Review." *International Journal of Transportation Science and Technology* 12 (1): 315–328. https://doi.org/10.1016/j.ijtst.2022.03.002.

Mussone, L., V. J. Aranda Salgado, and R. Notari. 2024. "Evaluation of Robustness in Underground Networks." *Physica A: Statistical Mechanics and Its Applications* 651:130014. https://doi.org/10.1016/j.physa.2024.130014.

Mussone, L., H. Viseh, and R. Notari. 2020. "A Topological Analysis of Underground Network Performance Under Disruptive Events." In *ETC2020*, Milan, 1–25, AET 2020.

Mussone, L., H. Viseh, and R. Notari. 2022. "Novel Centrality Measures and Applications to Underground Networks." *Physica A: Statistical Mechanics and its Applications* 589:126595. https://doi.org/10.1016/j.physa.2021.126595.

Newman, M. E. J. 2001. "Scientific Collaboration Networks. II. Shortest Paths, Weighted Networks, and Centrality." *Physical Review E* 64 (1): 016132. https://doi.org/10.1103/PhysRevE.64.016132.

Opsahl, T., F. Agneessens, and J. Skvoretz. 2010. "Node Centrality in Weighted Networks: Generalizing Degree and Shortest Paths." *Social Networks* 32 (3): 245–251. https://doi.org/10.1016/j.socnet.2010.03.006.

Scott, D. M., D. C. Novak, L. Aultman-Hall, and F. Guo. 2006. "Network Robustness Index: A New Method for Identifying Critical Links and Evaluating the Performance of Transportation Networks." *Journal of Transport Geography* 14 (3): 215–227. https://doi.org/10.1016/J.JTRANGEO.2005.10.003.

Stoilova, S., and V. Stoev. 2015. "Study of Passengers' Flow at Underground Stations." *Journal of Multidisciplinary Engineering Science and Technology (JMEST)* 2 (5): 1148–1154.

Tsiotas, D., and S. Polyzos. 2015. "Introducing a New Centrality Measure from the Transportation Network Analysis in Greece." *Annals of Operations Research* 227 (1): 93–117. https://doi.org/10.1007/s10479-013-1434-0.

Wang, F., A. Antipova, and S. Porta. 2011. "Street Centrality and Land Use Intensity in Baton Rouge, Louisiana." *Journal of Transport Geography* 19 (2): 285–293. https://doi.org/10.1016/j.jtrangeo.2010.01.004.

Wang, Y., and K. Cullinane. 2016. "Determinants of Port Centrality in Maritime Container Transportation." *Transportation Research Part E: Logistics and Transportation Review* 95:326–340. https://doi.org/10.1016/j.tre.2016.04.002.

Wang, Z., W. Ma, and A. Chan. 2020. "Exploring the Relationships Between the Topological Characteristics of Subway Networks and Service Disruption Impact." *Sustainability* 12 (10): 3960. https://doi.org/10.3390/su12103960.

Wang, J., H. Mo, F. Wang, and F. Jin. 2011. "Exploring the Network Structure and Nodal Centrality of China's Air Transport Network: A Complex Network Approach." *Journal of Transport Geography* 19 (4): 712–721. https://doi.org/10.1016/j.jtrangeo.2010.08.012.

Wong, K. I., S. Wang, C. O. Tong, W. Lam, H. Lo, H. Yang, and H. P. Lo. 2005. "Estimation of Origin-Destination Matrices for a Multimodal Public Transit Network." *Journal of Advanced Transportation* 39:139–168. https://doi.org/10.1002/atr.5670390203.

Wu, X., H. Dong, C. K. Tse, I. W. H. Ho, and F. C. M. Lau. 2018. "Analysis of Metro Network Performance from a Complex Network Perspective." *Physica A: Statistical Mechanics and Its Applications* 492:553–563. https://doi.org/10.1016/j.physa2017.08.074.

Xu, Q., B. H. Mao, and Y. Bai. 2016. "Network Structure of Subway Passenger Flows." *Journal of Statistical Mechanics: Theory and Experiment* 2016:033404. https://doi.org/10.1088/1742-5468/2016/03/033404.

Zhang, Q., X. Liu, S. Spurgeon, and D. Yu. 2021. "A Two-Layer Modelling Framework for Predicting Passenger Flow on Trains: A Case Study of London Underground Trains." *Transportation Research Part A: Policy and Practice* 151:119–139. https://doi.org/10.1016/j.tra.2021.07.001.